



Experimental Investigation of the Bonding Behavior of High-Volume Fly Ash Self-Compacting Concrete Reinforced with Steel and GFRP Bars

Waleed Awad Waryosh¹, Bilal Rasol^{1*}

¹Civil Engineering Department, Faculty of Engineering,
Al- Mustansiriyah University, Baghdad, 61102. IRAQ

*Corresponding Author

DOI: <https://doi.org/10.30880/ijscet.2023.14.04.022>

Received 13 March 2023; Accepted 13 December 2023; Available online 28 December 2023

Abstract: This paper investigated the bond strength between reinforcement steel and GFRP bars embedded in high-volume fly ash concrete and conventional concrete mixtures. This research evaluated two mixes: conventional concrete, and 50% replacement cement with Class F fly ash. According to RILEM recommendations, eight hinged beams were employed to evaluate the bond strength of the concrete mixes. This investigation showed good bonding for concrete mixes containing 50% fly ash compared to conventional concrete. GFRP bars also showed good bonding, better than steel bars in the case of small diameters (10 mm), but lower bonding in the case of larger diameters (16 mm).

Keywords: Reinforcement, GFRP, corrosion, bond behaviour, beam test, fly ash, failure

1. Introduction

The main issues with typical mild steel-reinforced concrete are carbon dioxide emissions and corrosion. Corrosion is a major issue that, if neglected for a long time, can lead to structural damage [1]. In the United States, there are roughly 600,000 bridges, of which 235,000 are constructed of steel-reinforced conventional concrete (Kessler and Powers 1988). Due to reinforcing corrosion, about 15% of them are considered structurally deficient. According to the National Association of Corrosion Engineers (NACE), the annual direct cost of corrosion is 8.3 \$ billion (Koch, Brongers et al. 2002). Glass fiber (GFRP) rebar has been used instead of steel reinforcement bars because of its lightweight and to minimize corrosion problems in concrete structures. Because of their great corrosion resistance and low cost, GFRP bars have gained a footing in the building industry during the last 25 years (Khalifa, Gold et al. 1998). Steel is 0.25 \$ per meter, whereas GFRP is 0.20 \$ per meter. GFRP reinforcing bars are about three times lighter than steel bars, thus reducing the cost of transportation and laborers (Skapa 2012). The second issue arises from conventional concrete, which uses only cement as a binder. The cement industry has expanded significantly all over the world in recent years. It is the third-largest carbon dioxide emitter in the world (Andrew 2018). Cement has been utilized as a binding construction material significantly, its popularity skyrocketed after WWII, with current global output levels equaling more than 500 kg per person annually (Andrew 2018). Several technologies have been proposed to replace Portland cement in concrete with a more environmentally friendly binding material. Fly ash, a byproduct of coal-burning thermal power plants, is one that has gained wide acceptance (Bilodeau and Malhotra 2000). The finely divided residue that follows from the burning of ground or powdered coal and is conveyed by flue gases," according to the definition of fly ash according to ASTM C618-08. Fly ash products are divided into three categories: class N, F, and C. Chemical compositions distinguish one from the other (Sideris, Justnes et al. 2018). Fly ash has been used in

*Corresponding author: bilalraasol@gmail.com

concrete structures just for 15-30% of the cement replacement (Berry, Hemmings et al. 1994). A previous study has demonstrated that replacing cement with a high replacement dosage of fly ash produces durable concrete.

HVFAC concrete is green and more sustainable alternative to Portland cement concrete. Fly ash costs 15\$ to 40\$ per ton, while Portland cement costs 50\$ to 70\$ per ton (Yuuml and ksel 2010). HVFAC is defined by ACI 232.2R as concrete mixes containing at least 50% fly ash(Sideris, Justnes et al. 2018). There has been a lot of research on the fresh and hardened properties of HVFAC, but there has been relatively little research on how it behaves structurally (Arezoumandi, Looney et al. 2015). Naik et al. (Naik, Singh et al. 1989) conducted pullout test on concrete specimens with different ratios of fly ash replacing cement and reported that the bond strength increases when the fly ash ratio was increased up to 20% in a pullout test. Gopalakrishnan et al. (Gopalakrishnan, Lakshmanan et al. 2005) conducted pullout tests on concrete with 50% replacement cement by fly ash, thus observed that the bond strength of the 50% fly ash was equivalent to ordinary concrete. Arezoumandi et al. (Arezoumandi, Looney et al. 2015) conducted another investigation into HVFAC concrete to evaluate the bond strength using a pullout test of steel reinforcing bar in HVFAC concrete with three proportions of fly ash in concrete mixes: 0.0 %, 50%, and 70% instead of Portland cement. They found that increases in fly ash percentage enhance the bond strength between the reinforcing bar and the concrete that surrounds it. Many researchers have conducted many investigations related to the bonding mechanism between GFRP bars and the surrounding concrete. Zenon Achillides and Kypros Pilakoutas (Achillides and Pilakoutas 2004) conducted a pullout test on GFRP bars implanted within concrete cube specimens, they found that the bond strength of GFRP was found to be comparable to that of steel bars. In general, the GFRP showed good bond behavior in all investigations with ultimate bond stress comparable to 85 % of the ultimate bond stress of steel reinforcing bars (Nanni, De Luca et al. 2014).

Pull-out test and the splice test are used in many studies to determine the bond behavior of GFRP reinforcing bar to concrete. The RILEM Institute (RILEM 1983) recommends the pullout and beam-bond tests as the best recognized and most frequently utilized techniques for bond testing. Direct pull-out testing on reinforced concrete members does not reflect the real bonding conditions in structural members. hinged beam bond test and reflect real bond behavior of the reinforcing bars with surrounding concrete in flexure reinforced concrete members.

The main objective of this investigation is to determine the bonding behavior of GFRP, and steel bars implanted in conventional concrete and high-volume fly ash concrete as sustainable concrete. This study used 50 % fly ash instead of cement, as well as two bar diameters of GFRP and steel, were used:10 mm and 16 mm.

2. Experimental Details

2.1 Specimen Fabrication

Among various, methods to investigate the bonding behavior of concrete and reinforcing bars is hinged beam testing. The test technique's primary premise is to apply flexural load to a test beam until the tested bar's total bond failure occurs in one-half of the beam or until the reinforcing bar itself ruptures (Seis and Beycioğlu 2017). During the test, the relative slip between concrete and the reinforcing bar is recorded. Hinged beam assists in determining the slip of the tested bars by applying the load at the midpoint in the tension zone. This methodology was chosen for this investigation because the beam test is more similar to real structural members and thus provides a better estimate of bond strength (especially for flexural members)(Pop, De Schutter et al. 2013). Eight beam specimens with dimensions of 100 x 200mm with a length of 820mm were used in the testing procedure. the implanted length was 10 times of bar diameter (10 Ø), and the rest of the bar was placed inside plastic sleeves to make a nonbonding length within the beam. The test beam is made up of two RC blocks connected at the bottom by GFRP or steel bar (10mm or 16mm diameter). To ensure that the tensile loads are distributed more accurately, a steel hinge is positioned at the mid-point of the beam as shown in Figure.1.

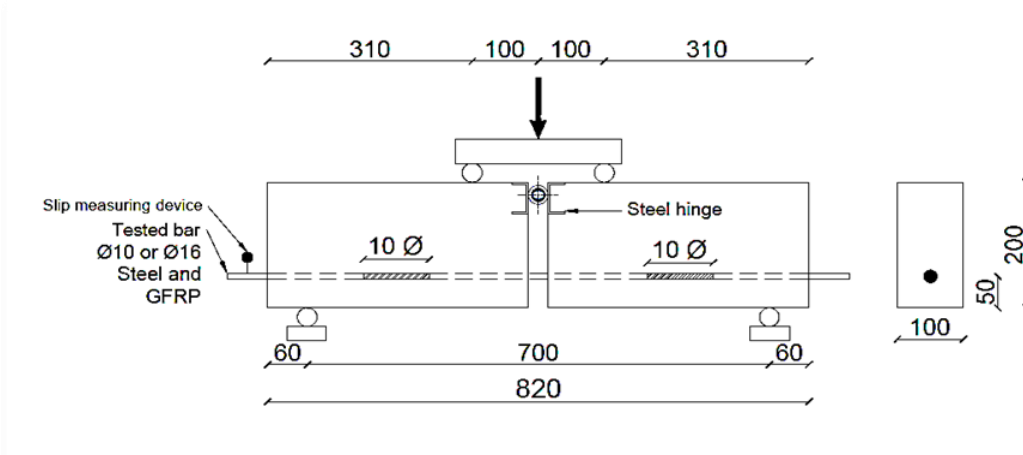


Fig. 1 - Dimensions and geometry of beams (Szczech and Kotynia 2018)

It is important to prevent shear cracks during loading, so stirrups with a diameter of 8 mm and a spacing of 70 mm were utilized to ensure the shear resistance of beam specimens (Szczech and Kotynia 2018). The bottom and top reinforcement consisted of two longitudinal steel bars (10 mm diameter). At the middle of the beam's height, there were an additional two steel bars with a 10 mm diameter, as illustrated in Figure.2.

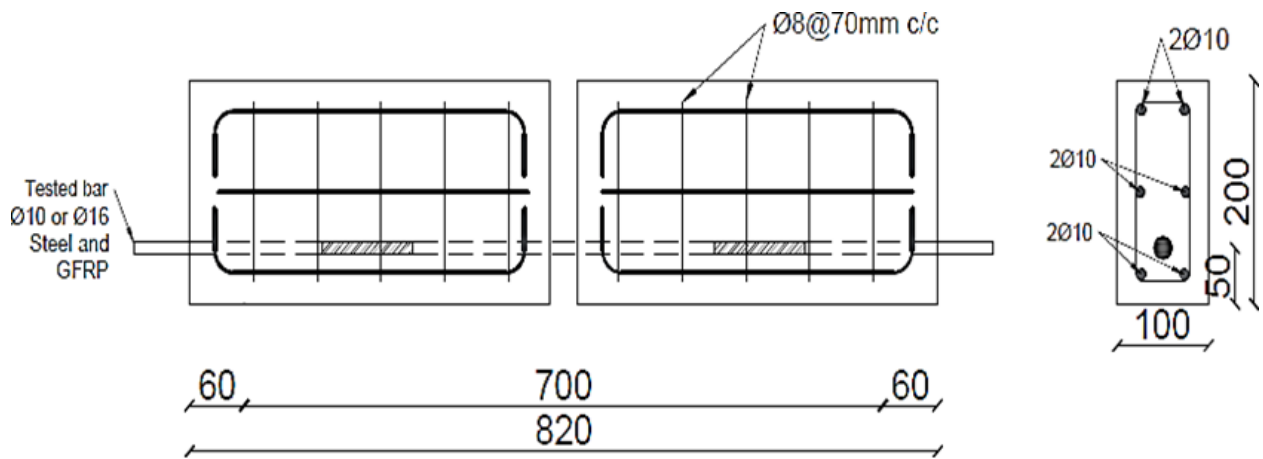


Fig. 2 - Reinforcement details of beam specimens

A nomenclature system with three symbols was used to describe the specimens that were tested, a nomenclature system is clarified as follows:

The first symbols denote the concrete type, the symbol (C) denotes that the specimen is from the conventional concrete category and the symbol (F50) denotes that the specimen belongs to high volume fly ash concrete category. It is always subscripted by the number (50), which represents the ratio of cement replacement by fly ash.

The second symbols denote the type of investigated bar, the symbol (S) denotes that the beam specimen reinforced with the steel bar, and (G) denotes that the beam specimen reinforced with GFRP bar. It is always subscripted by the number (10,16), which represents bar diameter in mm, Table.1 illustrate nomenclature system.

Table 1 - Nomenclature system

Specimen	Concrete Type	Rebar Type	Nominal Diameter (mm)
C-S ₁₀	Conventional concrete	Steel	10
C-S ₁₆		Steel	16
C-G ₁₀	High volume fly ash concrete	Glass Fiber	10
C-G ₁₆		Glass Fiber	16
F ₅₀ S ₁₀	High volume fly ash concrete	Steel	10
F ₅₀ S ₁₆		Steel	16
F ₅₀ G ₁₀	High volume fly ash concrete	Glass Fiber	10
F ₅₀ G ₁₆		Glass Fiber	16

2.2 Material Characteristics

2.2.1 Steel Bars

In this study, three steel bars with diameters of 8, 10, and 16 mm were used. Testing of these bars in tension machine at the College of Engineering, Al-Mustansiriyah University, the results shown in Table.2. The testing results for these steel bars were accordance with ASTM A615/A615M-09b (Astm 2009).

Table 2 - Tension results of Steel bars

Nominal Diameter (mm)	Yield Stress (MPa)	Ultimate Strength (MP)	Total elongation (%)
8	517	654	10
10	524	650	13
16	497	759	10.7

2.2.2 GFRB Bars

In this study, two different diameters of GFRP bars were used as longitudinal bars to evaluate the bonding with adjacent concrete. The mechanical properties of GFRB bars shown in Table .3.

Table 3 - Properties of GFRP bar

Bar diameter (mm)	Ultimate tensile Load (KN)	Guaranteed tensile strength (mpa)	Modules of elasticity (Gpa)
10	59	827	46
16	143	724	46

2.2.3 Cement

The cement used in this study was (Karesta Company) Portland Cement, symbol CEM II/ A-L. Tables .4 show the cement's physical and chemical properties. The test results of this cement meet IQ.S. 5:2019 specification (Kadhun and Haider 2020).

2.2.4 Fly Ash

The present investigation used Class F fly ash supplied by the " EUROBUILD " building chemicals company. The X-Ray Fuorescence (XRF) testing was carried out in accordance with BS EN 196-2-2013, and the outcomes of the test are shown in Table.4.

Table 4 - Physical and chemical properties of cementitious materials

Compositions	Ratio of compositions	Cement	Limitation IQ.S. NO.5:2019 (Jabal, Al- Baghdadi et al. 2021)	Fly Ash	Limits of ASTM C 618- 03(Diaz-Loya, Juenger et al. 2019)
SiO2	%	18.14		47.67	
Al2O3		6.71		27.73	Total ≥ 70%
Fe2O3		2.9		18.42	
Cao		60.74		5.11	
MgO		1.28	> 5	2.65	
SO3		2.09	> 2.8	3.71	≤5
Na2O		---		---	

K ₂ O		---		---	
Na ₂ O		---		---	
Loss in ignition		2.25	> 4	3.71	≤6
Fineness (Blaine)	Cm ² /gm	4678	< 2800	---	
C ₃ S		---		---	
C ₂ S		---		---	
C ₃ A		12.88		42.38	
C ₄ AF		---		---	
Initial set time	minute	125	≥45	---	
Final set time	hours	3.5	≤ 10	---	
Specific gravity		---		2.2	

2.2.5 Fine Aggregate

Natural sand is utilized as fine aggregate in this study for concrete mixes, and it has rounded-shaped particles with a smooth texture and a maximum size of 4.75mm. Sieve analysis is performed in accordance with the limitations of IOS No. 45/1984(No 1984).

2.2.6 Coarse Aggregate

Crushed gravel was utilized to cast the concrete samples, with a maximum size of 12 mm. physical and chemical properties are conducted in accordance with the limitations of IOS No. 45/1984 (No 1984).

2.2.7 Limestone Powder

The fine limestone powder is very effective in preventing excessive heat generation, improving fluidity and cohesion, improving segregation resistance, and increasing the quantity of fine powder in the mixes(Larsen and Naruts 2016).

2.2.8 Superplasticizers (Sika Viscocrete-5930)

It's a third-generation super plasticizing concrete admixture. Its base is an aqueous solution of modified polycarboxylate. The features of the superplasticizers (Sika Viscocrete-5930) utilized in this study meet ASTM standard specifications for categories G and F (ASTM C494/C494M, 2015).

2.3 Concrete Mixes

Two mixtures (high-volume fly ash concrete HVFAC and conventional concrete CC) were cast in this work to attain a compressive strength of 30 MPa after 28 days for (150*150*150 mm) cubes. For conventional concrete slump test was 50 mm according to (ASTM) C143 (ASTM 2012). High volume fly ash concrete is considered to be self-compacting concrete if its fresh proprieties are in accordance with the specification of EFNARC (EFNARC 2002).

Table 5 - Details mixes

Mix	Cement (kg/m ³)	Fly ash (kg/m ³)	Limestone (kg/m ³)	Fine aggregate (kg/m ³)	Coarse aggregate (kg/m ³)	Water (kg/m ³)	Superplasticizer (l/m ³)
Conventional concrete (Mohammed 2017)	400	---	---	600	1200	180	---
High volume fly ash concrete (Taha 2019)	200	200	100	840	800	170	5.4

Table 6 - Test results of fresh high-volume fly ash self-compacting concrete

Test	Property	Unit	Test results	Range
Slump flow		mm	750	650-800
T ₅₀	Filling ability	sec	3	2-5
V-funnel	Segregation resistance	sec	9	6-12
L-box	Pass ability	%	0.9	0.8-1

Table 7 - Mechanical properties of hardened concrete

Mix	Compressive Strength		Rupture Modulus (<i>f_r</i>) (mpa)	Splitting Tensile Strength (<i>f_{ct}</i>) (mpa)	Elasticity Modulus (<i>E_c</i>) (GPa)
	<i>f_{cu}</i> (mpa)[31]	<i>f'_c</i> (mpa)			
Conventional concrete	32.5	28.3	4	2.98	24.2
High volume fly ash concrete	36	30.24	4.5	3.5	23

2.4 Experimental Set-up

The instruments were used to determine the bond behavior of beam specimens, these instruments are utilized to record the values of load and relative movement (slip) between the tested reinforcing bar surrounding concrete at every stage of loading. All beam specimens were tested using a hydraulic ELE flexural test machine in The Construction Material Laboratory college of Engineering, Mustansiriyah University.

The beam samples are put under a two-point load on the test machine and balanced according to the required span between the support point loads, the dial gauges are set at their proper positions, as shown in Figure 3.



Fig. 3 - Testing Set-up of the Beam Specimen under test machine

3. Test Results

3.1 Bond Stress Test

The ultimate pullout force in the tested rebar (*P_u*) was computed according to the value of maximum load (*F_{max}*).

$$P_u = \frac{F_{max} \times a}{2 \times b} \quad (1)$$

Where *P_u* is a pull-out force to the tested bar (KN); *F* is maximum applied load (KN); *a* is the shear span (mm); *b* is the lever arm from the center of the steel hinge to the center of the tested bar (mm). Then the ultimate bond stress of the tested bar (*τ_u*), is calculated based on the pull-out force *P_u* and bonded length (*π.Ø. L_b*) this concept is illustrated in Figure .4.

$$\tau_u = \frac{P_u}{\pi \cdot \phi \cdot L_b} \quad (2)$$

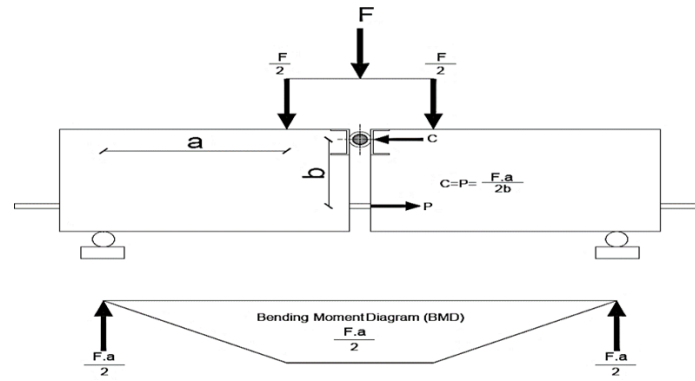


Fig. 4 - Pull-out force calculation according to the RILEM concept in the deformed bar

Table 8 - Results and mode failure

Specimens	Ø (mm)	Fmax (KN)	Slip (mm)	τ0.01 (mpa)	τ0.1 (mpa)	τ0.4 (mpa)	τu (mpa)	Mode Failure
C-S ₁₀	10	44.66	1.4	7.04	10.1	11.63	13.66	Pull-out
C-G ₁₀		51.07	1.3	7.35	12.25	14.5	15.63	Pull-out
F ₅₀ S ₁₀		49.5	0.75	6.13	12.3	18	18.6	Bar Rupture
F ₅₀ G ₁₀		60.8	0.9	9.2	14.7	17.44	19.1	Bar Rupture
C-S ₁₆	16	65.84	1.2	3.3	5.38	7.42	7.87	Splitting
C-G ₁₆		60.7	0.9	3	6.09	7	7.3	Pull-out
F ₅₀ S ₁₆		116.74	1.1	6.46	12.4	13.51	13.95	Splitting
F ₅₀ G ₁₆		99.52	1.2	5.61	10.53	11.6	11.9	Splitting

τu: ultimate bond stress (bond stress at failure).

τ0.01: bond stress at slip 0.01 mm.

τ0.1: bond stress at slip 0.1 mm.

τ0.4: bond stress at slip 0.4 mm.

3.2 Bond Failure Mechanism

The mode of failure observed for every hinged beam is listed in Table .8. In the case of specimens poured with conventional concrete, pull-out failure was observed in GFRP 10 mm and 16 mm diameters, as shown in Figures (6.8). For steel bars, pullout failure was observed with a 10 mm diameter, but with a 16 mm diameter, split failure with micro-cracks was observed, as shown in Figures (5.7).

In specimens poured with a high volume of fly ash concrete, bar rupture occurred unexpectedly in both steel and GFRP (10 mm in diameter) as shown in Figures (9.10). But, for steel and GFRP specimens with a diameter of 16 mm, splitting failure has been observed within the bonding length as shown in Figures (11.12).

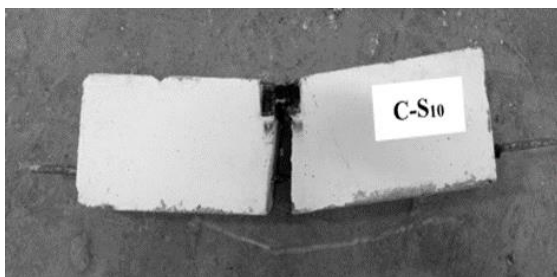


Fig. 5 - Pullout failure of steel bar 10 mm within conventional concrete

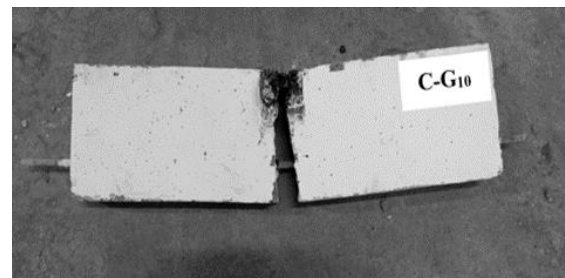


Fig. 6 - Pullout failure of GFRP bar 10 mm within conventional concrete

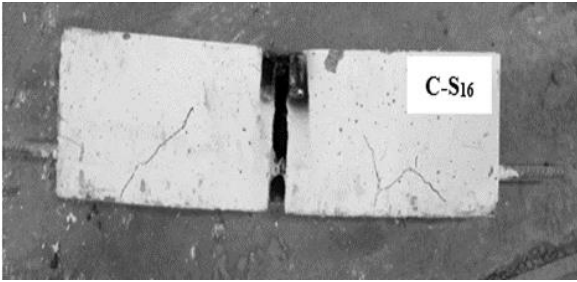


Fig. 7 - Splitting failure of steel bar 16 mm within conventional concrete

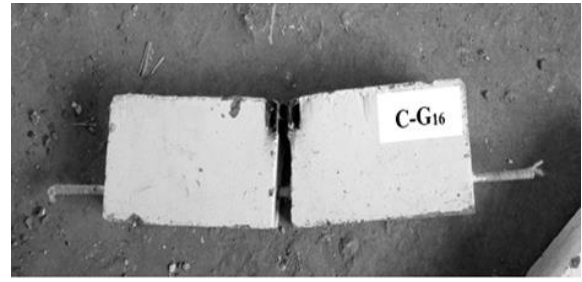


Fig. 8 - Pullout failure of GFRP bar 16 mm within conventional concrete

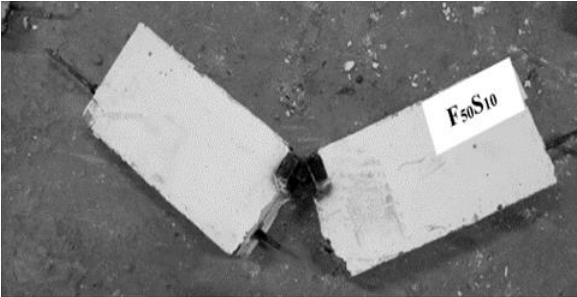


Fig. 9 - Bar rupture failure of steel bar 10 mm within high-volume fly ash concrete

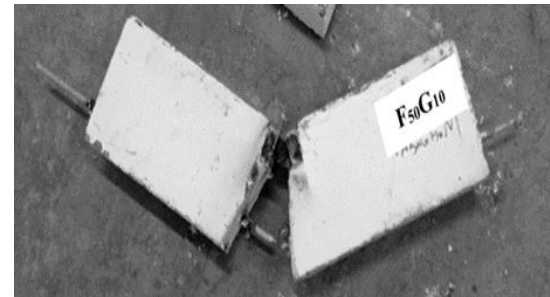


Fig. 10 - Bar rupture failure of GFRP bar 10mm within high-volume fly ash concrete

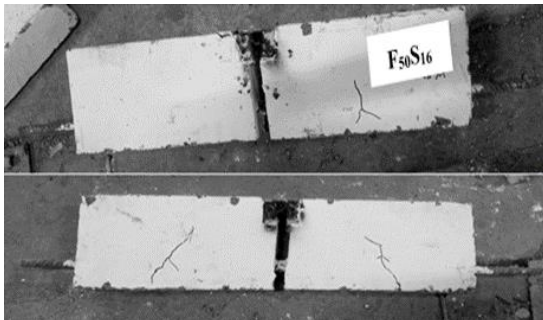


Fig. 11 - Splitting failure of steel bar 16 mm within high-volume fly ash concrete

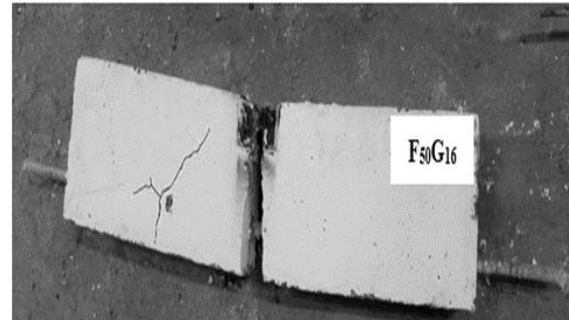


Fig. 12 - Splitting failure of GFRP bar 16 mm within high-volume fly ash concrete

3.3 Effect of Investigated Parameters on Bond Strength

3.3.1 Effect of Bar Type (Replacement Steel Bar by GFRP Bar)

In general, the results showed that small diameters of GFRP, provides ultimate bond strength (τ_u) higher than the bond stress of deformed steel bars this may be due to the roughness of GFRP bar surface (sand coated). For conventional concrete with a diameter of 10 mm, GFRP bars showed an ultimate bond stress higher than steel bars by 18.8%. Also, high-volume fly ash concrete with a diameter of 10 mm, the GFRP bar showed an increase in bond strength by 2.7% more than steel bar for same diameter. The results and other researchers (Szczech and Kotynia 2018) indicated that bond strength for GFRP bars was relatively lower than that of deformed steel bar, in contrast to small diameters. The bond strength of GFRP bar in conventional concrete and high volume fly ash concrete with the same diameter (16mm) was 7.3% and 13.4% lower than that of steel bar, respectively.

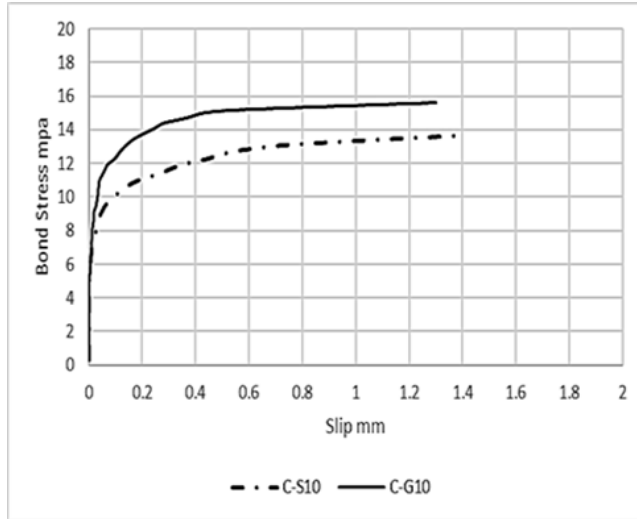


Fig. 13 - Bond –slip relationship of 10 mm diameter within conventional concrete

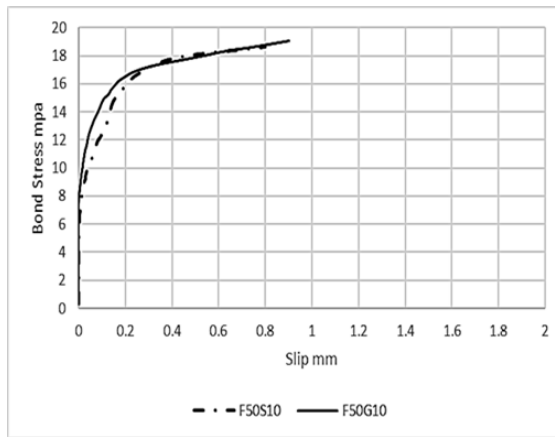


Fig. 14 - Bond – slip relationship of 10 mm diameter (steel/GFRP) within conventional concrete

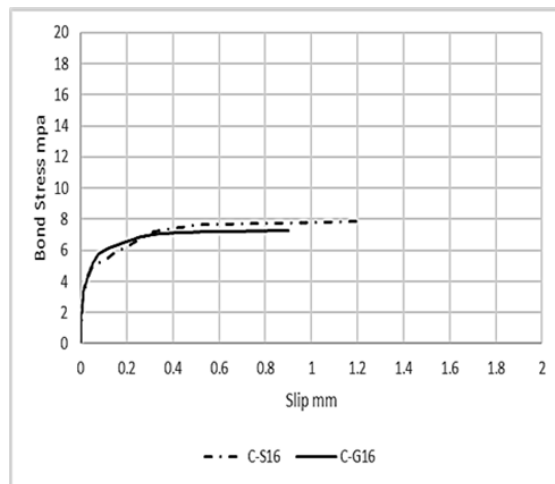


Fig. 15 - Bond –slip relationship of 10 mm diameter (steel/GFRP) within conventional concrete

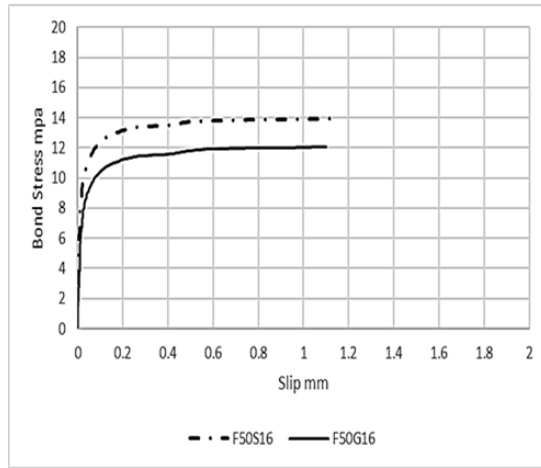


Fig. 16 - Bond – slip relationship of 10 mm diameter (steel//GFRP) within high-volume fly ash concrete

3.3.2 Effect of Bar Diameter

According to the result of this investigation, the bonding stresses decrease as the diameter of the reinforcing bar increases. For steel bars embedded in conventional concrete, the bonding stresses reduce by 40.2% as the diameter increases from 10mm to 16mm, it also decreases by 53.3% for GFRP bar when comparing 16 mm diameter in relation to 10 mm diameter. The bonding stress of steel bars implanted in high-volume fly ash concrete decreases by 25 % when the diameter of the reinforcing steel rebar diameter increases (10 to 16 mm). Also, bonding stress decreases by 36.8% when comparing the different diameters for GFRP bars.

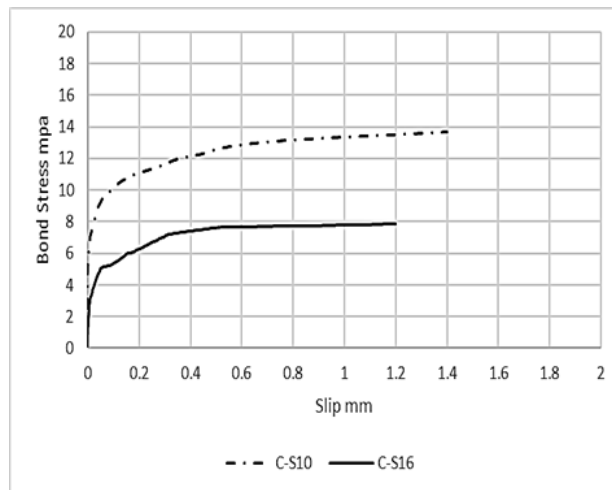


Fig. 17 - Bond-slip relationship of steel bars with diameters (10mm&16mm) in conventional concrete

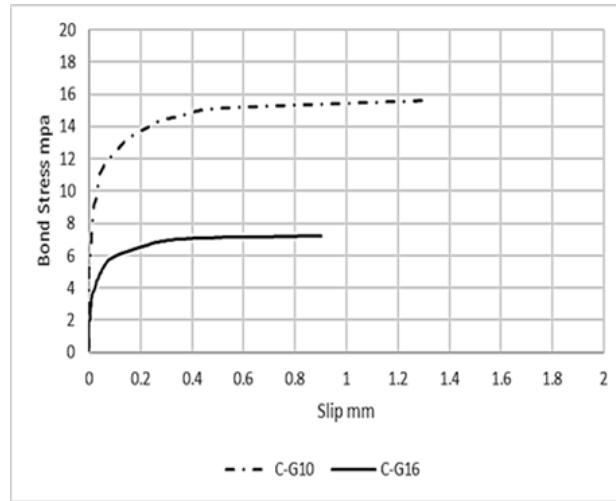


Fig. 18 - Bond-slip relationship of GFRP bars with diameters (10mm&16mm) in conventional concrete

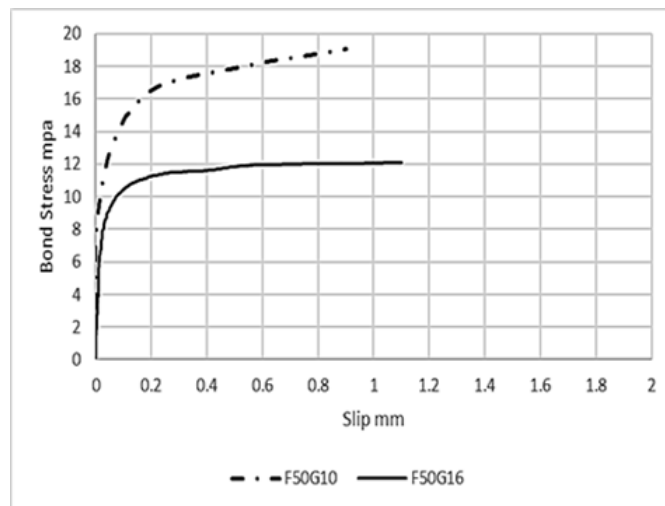


Fig. 19 - Bond-slip relationship of steel bars with diameters (10mm&16mm) in high-volume fly ash concrete

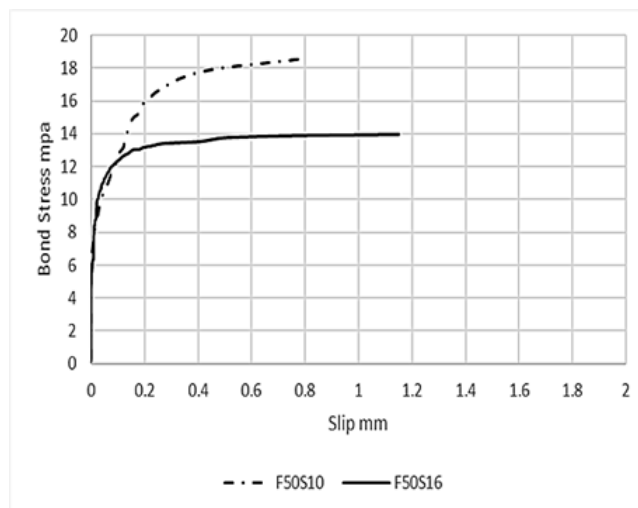


Fig. 20 - Bond-slip relationship of GFRP bars with (10 mm&16mm) in high-volume fly ash concrete

3.3.3 Effect of A Concrete Type (Replacement Cement by Fly Ash)

One of the parameters in this research is the effect of replacement fly ash instead of Portland cement on the bond strength of steel and GFRP bars. The results showed that the bond stress of steel bars (diameter 10 mm) in high-volume fly ash concrete increased by 41.4 % more than that embedded in normal concrete with the same diameter. It was also found that the bonding stresses for GFRP bars (10 mm) surrounded by high volume fly ash concrete increased by 22.2% compared to conventional concrete. It has also been shown that steel bars (16 mm) embedded within high-volume fly ash concrete showed bond stress 77.3% higher than conventional concrete for the same diameter. When GFRP bars (16 mm) were embedded in high-volume fly ash concrete, the bonding stress was 65.5 % higher than when embedded in conventional concrete.

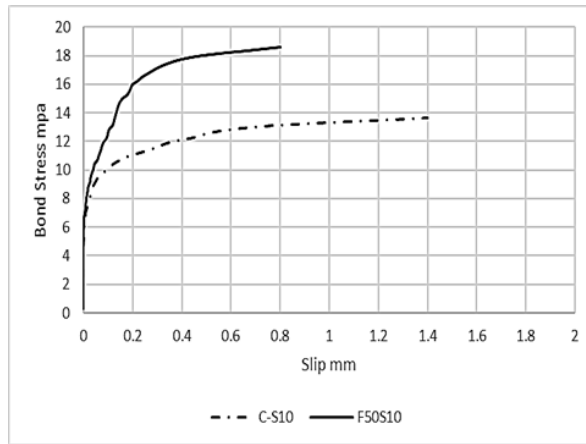


Fig. 21 - Bond-slip relation of steel bars with diameter (10mm) in conventional and high-volume fly ash concrete

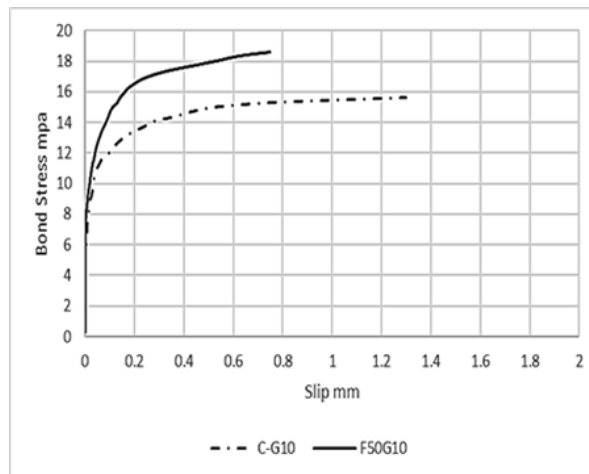


Fig. 22 - Bond-slip relation of GFRP bars with a diameter (10mm) in conventional and high-volume fly ash concrete

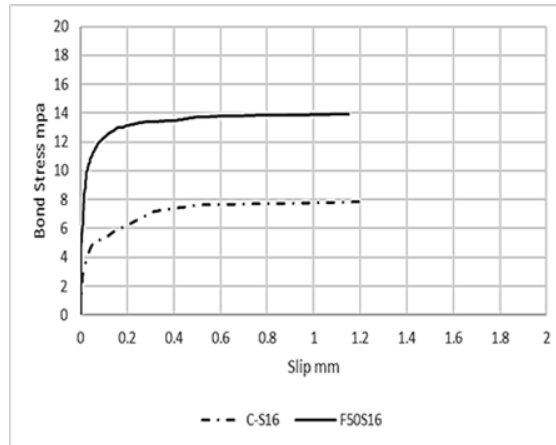


Fig. 23 - Bond-slip relation of steel bars with diameter (10 mm) in conventional and high-volume fly ash concrete

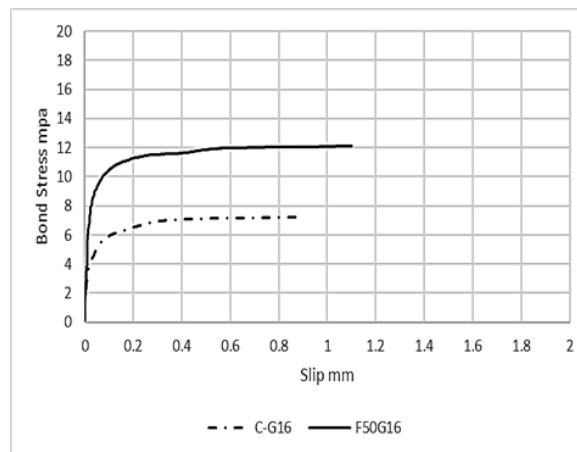


Fig. 24 - Bond-slip relation of GFRP bars with a diameter (10 mm) in conventional and high-volume fly ash concrete

4. Conclusions

This paper discusses the results of testing hinged beams reinforced with steel or GFRP bars. The investigated parameters were bar type (replacement steel by GFRP), concrete type (replacement cement by fly ash), and reinforcing bar diameter. In the case of small diameters (10 mm), the bond strength of GFRP bars is greater than that of steel bars for the same diameter, but the bond strength of GFRP bars for larger diameters (16 mm) is found to be slightly lower than that of steel bars.

In conventional concrete CC and high-volume fly ash concrete HVFAC, the bond strength of steel and GFRP bars decreased with increasing bar diameter, this drop rate was higher in GFRP bars due to the separation of sand grain on the GFRP surface. High-volume fly ash concrete HVFAC beams in this study showed higher bond strength compared with conventional concrete CC because of self-compacting properties that provide high adhesion with the reinforcing bar, as well as this mixture has more fine materials, so there are no voids between the tested bar and the concrete matrix that surrounds it. For GFRP bars embedded in conventional concrete CC, Pull-out failure was observed for small and greater diameters with sudden failure due to accelerated slip relative to the concrete that surrounds. Splitting micro cracks were observed in the bonding zone (bond length) only with large diameters (16 mm) embedded in both high-volume fly ash concrete HVFAC and conventional concrete CC. A faster slip has occurred with the onset of micro-splitting cracks in the bond length. The rupture of a 10 mm diameter steel and GFRP rebar in high-volume fly ash concrete occurred unexpectedly, this may be due to the high bonding provided by high-volume fly ash self-compacting concrete.

Acknowledgement

The authors would like to thank the staff of Mustansiriyah University, Baghdad, Iraq, for their support in the present work.

References

- Achillides, Z. and K. Pilakoutas (2004). "Bond behavior of fiber reinforced polymer bars under direct pullout conditions." *Journal of Composites for construction* 8(2): 173-181.
- Andrew, R. M. (2018). "Global CO₂ emissions from cement production." *Earth System Science Data* 10(1): 195-217.
- Arezoumandi, M., et al. (2015). "Effect of fly ash replacement level on the bond strength of reinforcing steel in concrete beams." *Journal of Cleaner Production* 87: 745-751.
- ASTM, C. (2012). "Standard test method for slump of hydraulic-cement concrete." ASTM International West Conshohocken, PA.
- Astm, S. (2009). "Standard specification for deformed and plain carbon-steel bars for concrete reinforcement, ASTM A615/A615M-09b." Search in.
- Berry, E. E., et al. (1994). "Hydration in high-volume fly ash concrete binders." *Materials Journal* 91(4): 382-389.
- Bilodeau, A. and V. M. Malhotra (2000). "High-volume fly ash system: concrete solution for sustainable development." *Materials Journal* 97(1): 41-48.
- Diaz-Loya, I., et al. (2019). "Extending supplementary cementitious material resources: Reclaimed and remediated fly ash and natural pozzolans." *Cement and concrete composites* 101: 44-51.
- EFNARC, F. (2002). "Specification and guidelines for self-compacting concrete." European federation of specialist construction chemicals and concrete system.
- Gopalakrishnan, S., et al. (2005). "Demonstration of utilising high volume fly ash based concrete for structural applications." Structural Engineering Research Centre, Chennai India.
- Jabal, Q., et al. (2021). Mechanical properties and durability for concrete using waste heat resistance glass (Pyrex Type) as coarse aggregate. *Journal of Physics: Conference Series*, IOP Publishing.
- Kadhun, A. O. and M. O. Haider (2020). "Experimental Investigation of Self-Compacting High Performance Concrete Containing Calcined Kaolin Clay and Nano Lime." *Civil Engineering Journal* 6(9): 1798-1808.
- Kessler, R. and R. Powers (1988). Corrosion of Epoxy Coated Rebar, Keys Segmental Bridges, Monroe County, Florida Department of Transportation, Materials Office.
- Khalifa, A., et al. (1998). "Contribution of externally bonded FRP to shear capacity of flexural members." *ASCE-Journal of Composites for Construction* 2(4): 195-203.
- Koch, G. H., et al. (2002). Corrosion cost and preventive strategies in the United States, United States. Federal Highway Administration.
- Larsen, O. A. and V. V. Naruts (2016). "Self-compacting concrete with limestone powder for transport infrastructure." *Magazine of Civil Engineering*(8 (68)): 76-85.
- Mohammed, M. (2017). "Reinforced Concrete Strengthening by Using Geotextile Reinforcement for Foundations and Slabs." Master of Science in Civil Engineering, Civil Engineering Department, Faculty of Engineering, Al-Mustansiriayah University.
- Naik, T. R., et al. (1989). "Concrete compressive strength, shrinkage and bond strength as affected by addition of fly ash and temperature." The University of Wisconsin–Milwaukee, Milwaukee, WI.
- Nanni, A., et al. (2014). "Reinforced concrete with FRP bars." *Mechanics and design, international standard book no-13*: 978-970.
- No, I. (1984). "45, Iraqi Specification," *Aggregate from Natural Sources for Concrete and Construction*. Central Agency for Standardization and Quality Control.
- Pop, I., et al. (2013). "Bond between powder type self-compacting concrete and steel reinforcement." *Construction and Building Materials* 41: 824-833.
- RILEM, T. (1983). "RC 6: Bond test reinforcing steel, 2, pull-out test." London (UK): E & FN SPON.
- Seis, M. and A. Beycioğlu (2017). "Bond performance of basalt fiber-reinforced polymer bars in conventional Portland cement concrete: A relative comparison with steel rebar using the hinged beam approach." *Science and engineering of Composite Materials* 24(6): 909-918.
- Sideris, K., et al. (2018). Fly ash. Properties of fresh and hardened concrete containing supplementary cementitious materials, Springer: 55-98.
- Skapa, S. (2012). "Investment characteristics of natural monopoly companies." *Journal of Competitiveness* 4(1).
- Szczuch, D. and R. Kotynia (2018). "Beam bond tests of GFRP and steel reinforcement to concrete." *Archives of Civil Engineering* 64(4/II).
- Taha, A. (2019). "Performance of high-volume fly ash self-compacting concrete exposed to external sulfate attack." Yuuml and E. ksel (2010). "The effect of cure conditions and temperature changes on the compressive strength of normal and fly ash-added concretes." *International Journal of Physical Sciences* 5(17): 2598-2604.